Supplementary Information

"Coupling of Nitroxyl Radical as Electrochemical Charging Catalyst and Ionic Liquid for Calcium Plating/Stripping toward a Rechargeable Calcium-Oxygen Battery"

Tohru Shiga,* Yuichi Kato, and Yoko Hase
Toyota Central Research & Development Laboratories Inc.

1. Materials

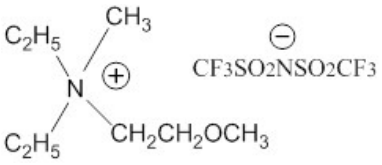

(DEMETFSA)

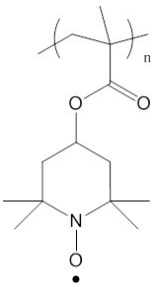

(PTMA)

Figure S1. Chemical structure

Table SI. Materials composition of cathode

Sample	PTMA	Ketjen black	Calcium oxide	Teflon binder
No.1	23.5	32.1	35.4	9.1
No.2	0	35.6	55.1	9.3
No.3	24.5	64.6	0	10.9

(% by weight)

2. Experimental

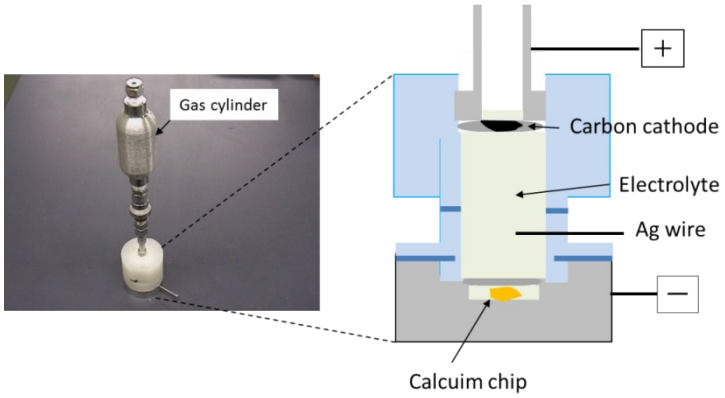

Figure S2. Schematic illustration of Air-cell

3. Results

3.1 Gas analysis

GC/MS spectra of the samples after electrochemical CaO decomposition test are shown in Figure S3. The gas cylinders involved nitrogen which was caused by the air involved at injection of sample gas into GC/MS spectrometer. Therefore, the amount of oxygen due to CaO decomposition was corrected by subtracting the contribution of air from the amount of oxygen measured by GC/MS.

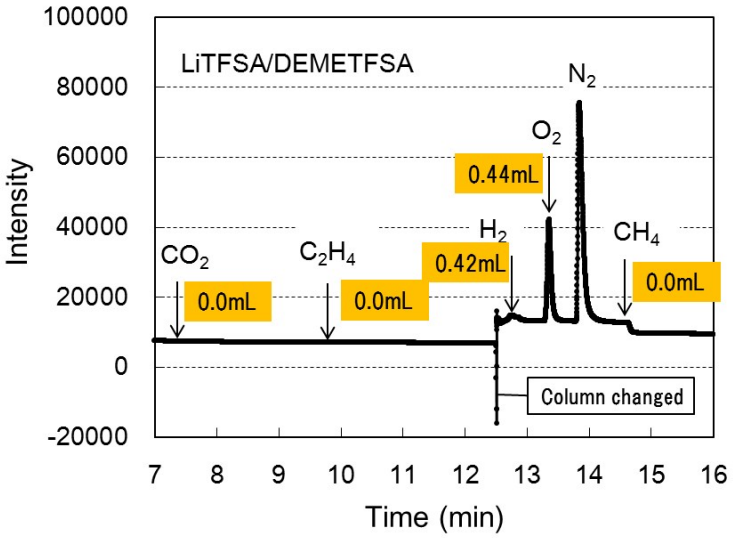

(a) LiTFSA/DEMETFSA

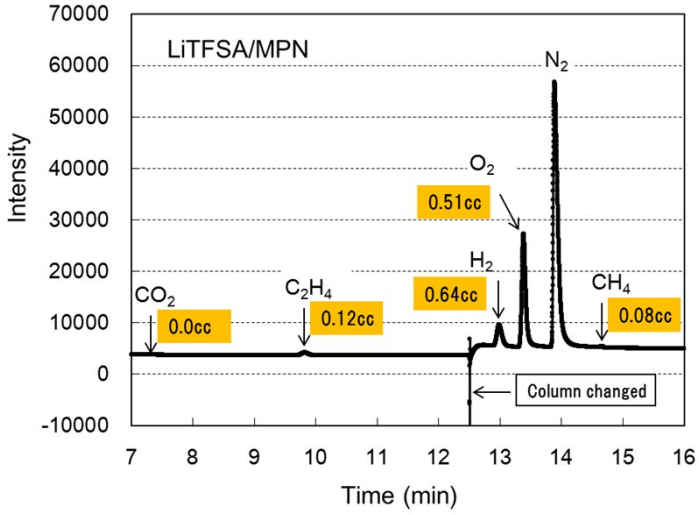

(b) LiTFSA/MPN

Figure S3. GC/MS spectra after electrochemical CaO decomposition test

3.2 CV curves of $Ca(TFSA)_2$-DEMETFSA electrolyte at 60 °C

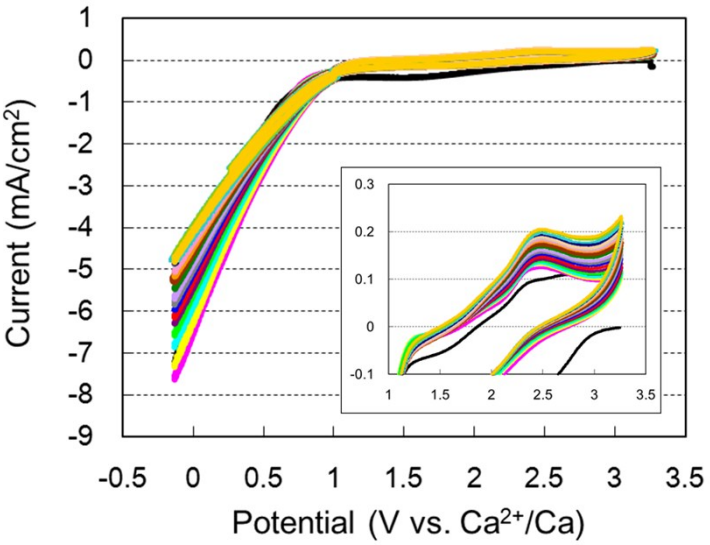

(a) Sweeping rate : 50 mV/sec

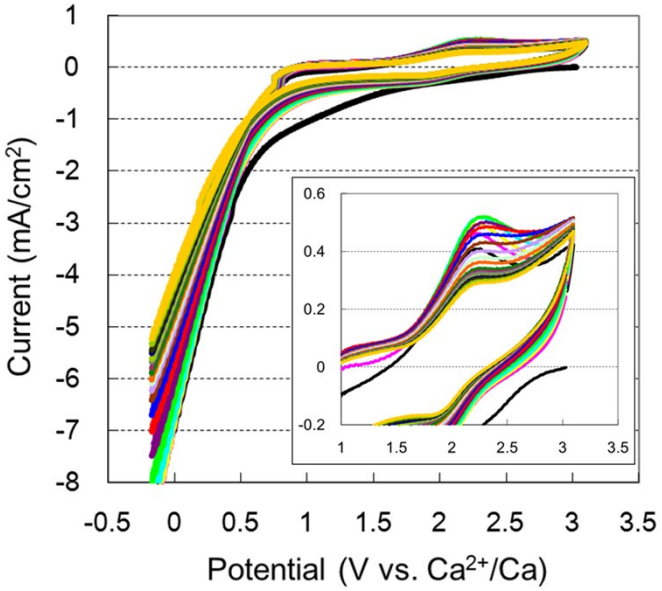

(b) Sweeping rate : 200 mV/sec

Figure S4. CV curves of $Ca(TFSA)_2$-DEMETFSA electrolyte at 60 °C

3.3 Photographs of Ca chips and quartz cell

(a) (b)

Figure S5. Photographs of Ca chips before (left) and after (right) immersing into the DEMETFSA electrolyte (a), and the quartz cell (b)

3.4 Raman spectral line assignment

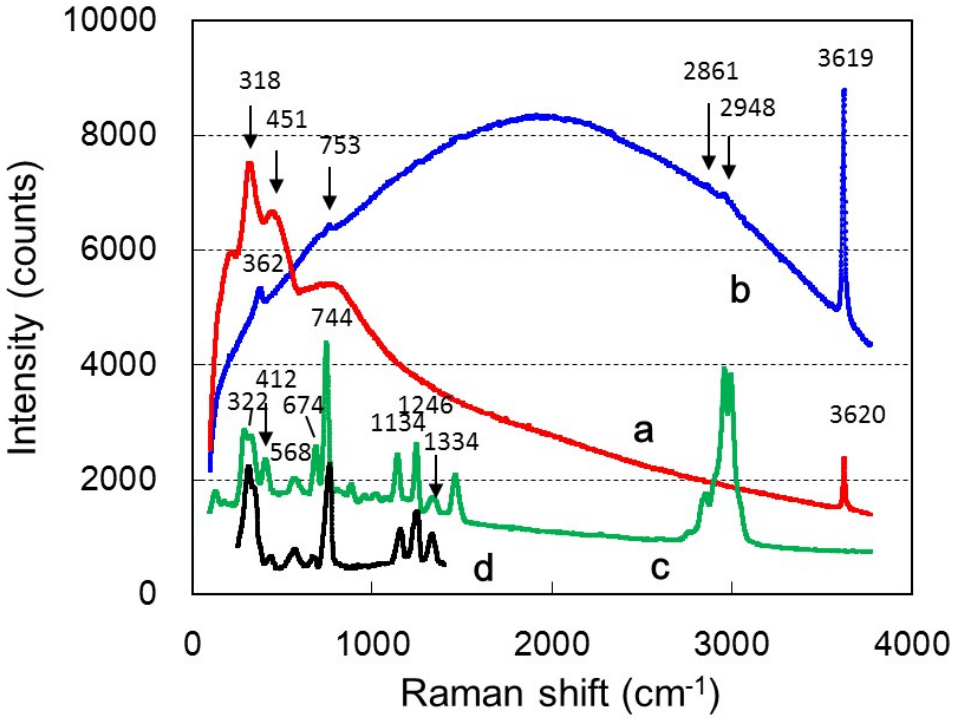

Figure S6. Raman spectra of (a) the SEI on Ca chips in DEMETFSA, (b) the SEI in MPN, (c) DEMETFSA, and (d) $Ca(TFSA)_2$.

3.5 TOF-SIMS spectra for negative ions

Surface analysis of Ca on Pt plate in $Ca(TFSA)_2$-DEMETFSA electrolyte was made by TOF-SIMS technique. The TOF-SIMS spectrometer was directly conducted through transfer chamber to an argon glove box in order to avoid moisture exposure of the sample. Three signals derived from DEME were detected at m/z = 116, 132, and 146.

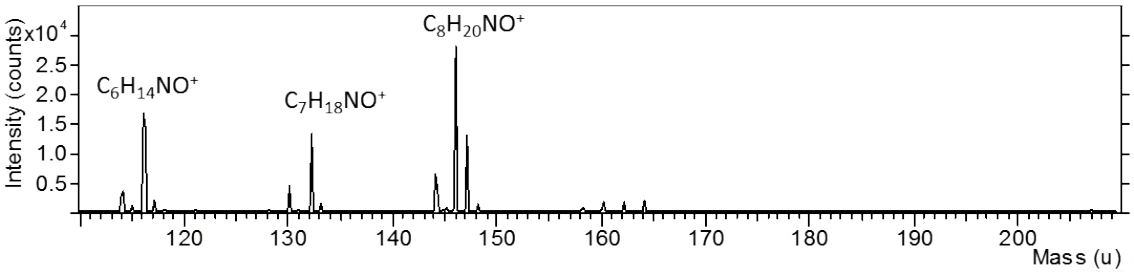

Figure S7. TOF-SIMS spectrum of Ca-deposited Pt plate in DEMETFSA electrolyte

3.6 Cell performance of Ca-O_2 cell using $Ca(TFSA)_2$-DEMETFSA electrolyte at 60 °C

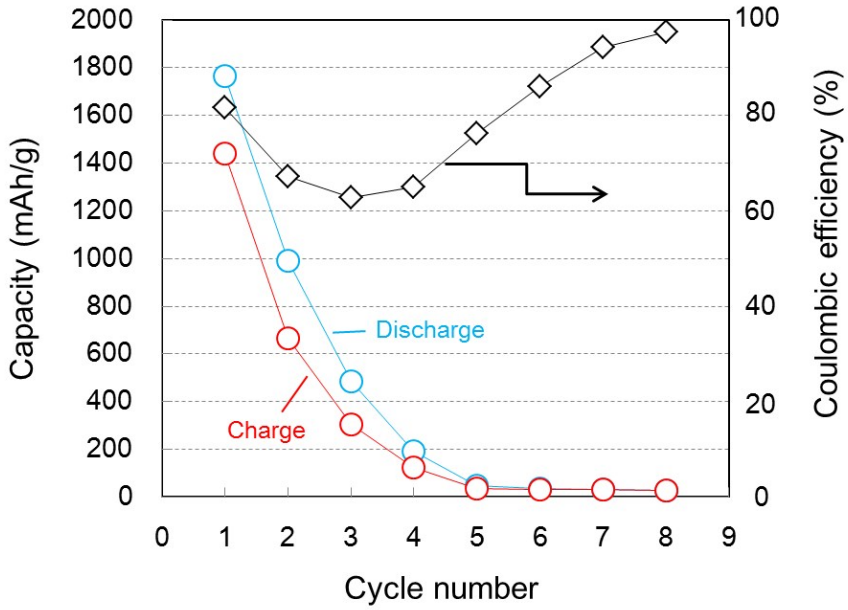

Figure S8. Cycle performance of Ca-O_2 cell using $Ca(TFSA)_2$-DEMETFSA electrolyte at 60 °C**.**

Discharge-charge curves at the 1st cycle under various discharge/charge currents were displayed in Figure S9. The upper limit of operation for the Ca-O_2 cell was 0.25mA/cm^2. This is because oxygen molecules diffuse slowly in high viscous electrolyte. Therefore, the supply of oxygen cannot keep up at air electrode.

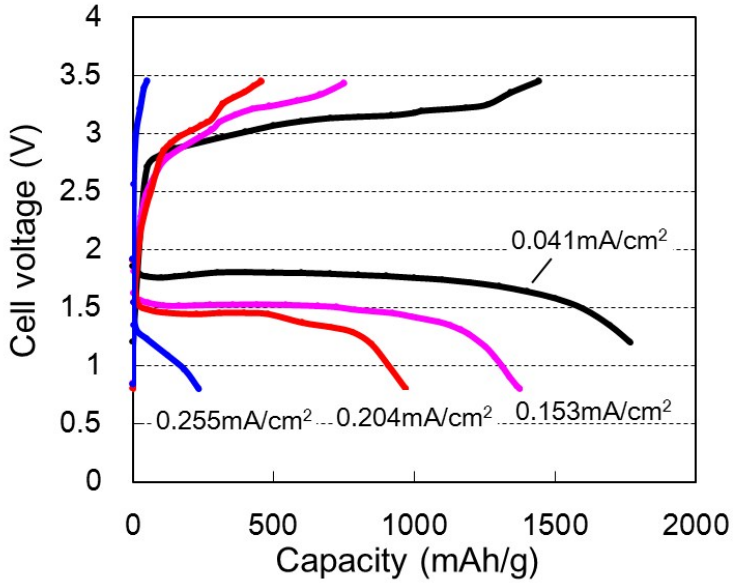

Figure S9. Rate performance of Ca-O_2 cell

3.7 Cycle performance of PTMA/Li and PTMA/Ca cells at 60 °C

We fabricated two types of radical battery, i.e., PTMA/LiTFSA-DEMETFSA/Li cell and PTMA/Ca(TFSA)$_2$-DEMETFSA/Ca cell. Charging was started under argon at at 60 °C.

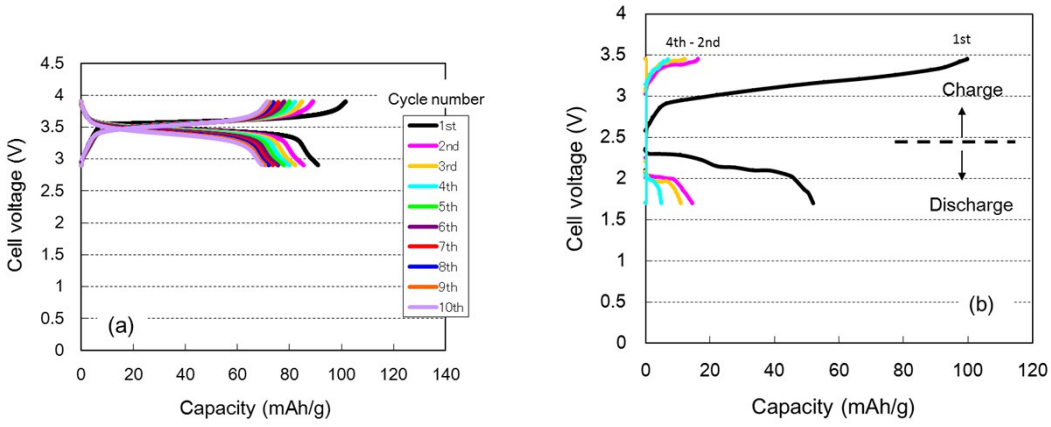

(a) PTMA/Li cell (b) PTMA/Ca cell

Figure S10. Cycle performance of the PTMA/Li and PTMA/Ca cells at 60 °C**.**
The electrolytes used were (a) LiTFSA-DEMETFSA, and (b) Ca(TFSA)$_2$-DEMETFSA.

3.8 Estimation of the contribution rate of the Ca anode to capacity fading at 60 °C

After the 3rd discharge/charge cycle under 0.154 mA/cm^2 was finished, the anode in Ca-O_2 battery was replaced with fresh Ca chips. We restarted the discharge/charge cycle test at 60 °C. The discharge capacity recovered to 67 % of the 1st cycle (red line).

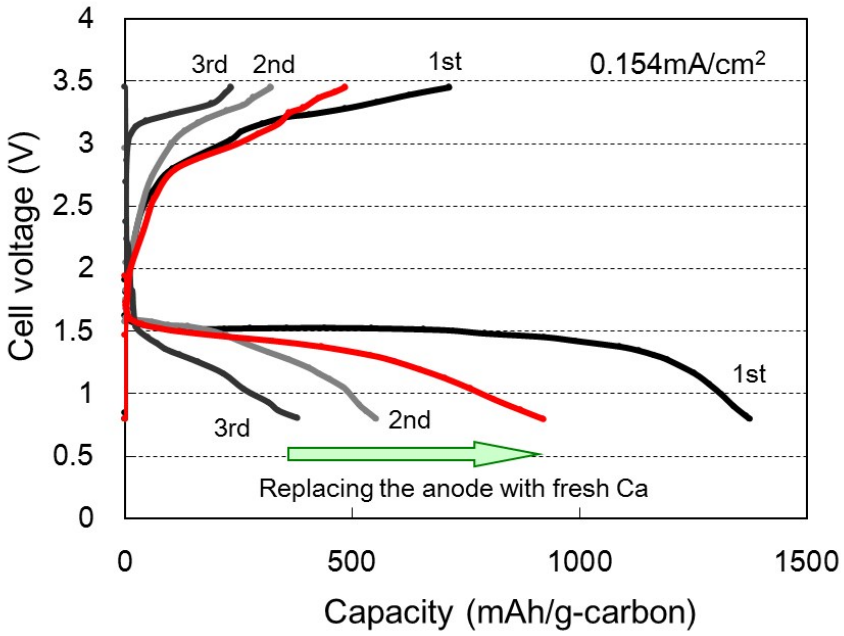

Figure S11. Effect of renewing Ca anode

3.9 Photographs of the cathodes after charge/discharge cycle test

(a) After the 1st discharge

(b) After the 1st charge

(c) After the 5th discharge

Figure S12. Photographs of the cathodes after charge/discharge cycle test

3.10 Characterization of the white precipitates on the cathode after discharge

White precipitates were observed at cathode of Ca-O_2 battery using $Ca(TFSA)_2$-DEMETFSA electrolyte after discharge. They were characterized by Raman and XPS techniques. As shown in Figure S12a, calcium peroxide was not detected. Calcium oxide was not activated by Raman spectroscopy. The XPS profiles are described in Figure S13. The XPS signals for Ca-2p and O-1s photoelectrons were detected after discharge.

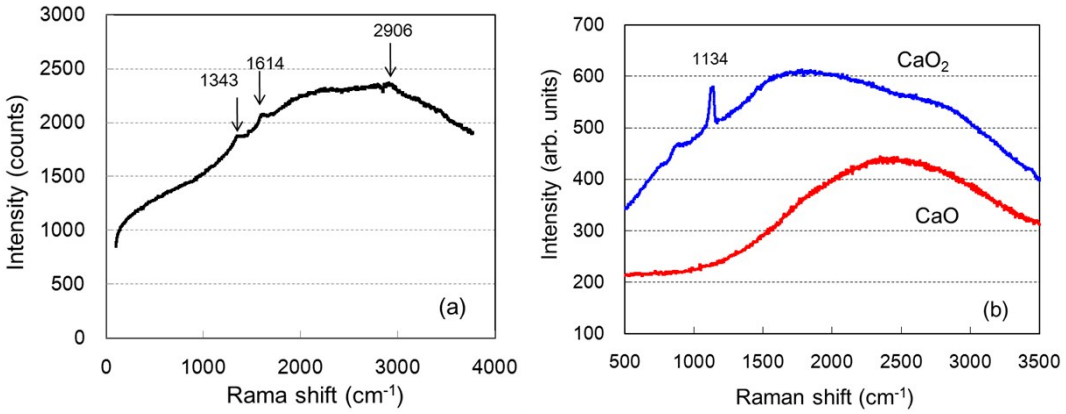

Figure S13. Raman spectra of (a) the white precipitates, and (b) Reagents of CaO and CaO_2

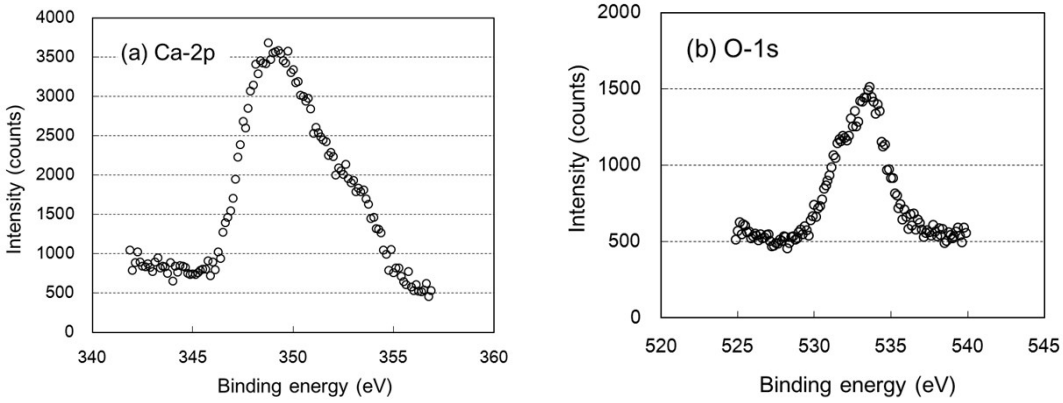

Figure S14. XPS profiles of the white precipitates on the cathode after discharging.

3.11 Gas analysis after charging

We exchanged from oxygen to argon in the gas cylinder after discharging Ca-O_2 battery using $Ca(TFSA)_2$-DEMETFSA electrolyte (discharge: 1945 mAh/g), and started charging (charge: 1380 mAh/g). We conducted a GC/MS test on the gas after charging.

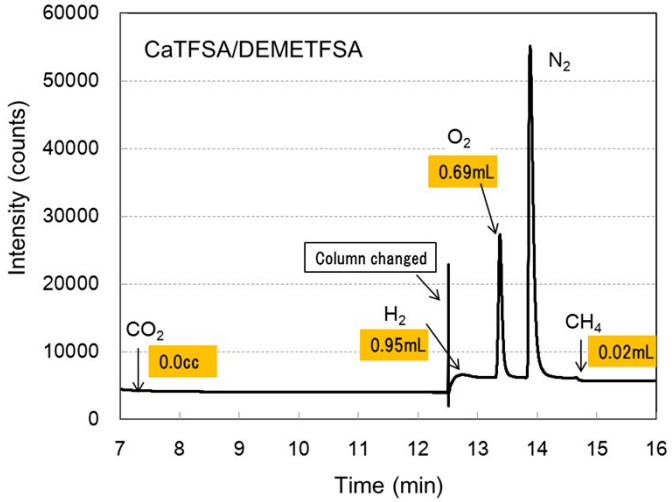

Figure S15. GC/MS profiles after charging the cell with gas cylinder by filling argon

3.12 Discharge/charge cycles of Ca-O_2 battery using $Ca(ClO_4)_2$-DEMETFSA electrolyte

We fabricated a Ca-O_2 battery using $Ca(ClO_4)_2$-DEMETFSA electrolyte to investigate the effect of anion of cell performance. The Ca-O_2 battery worked as a primary cell.

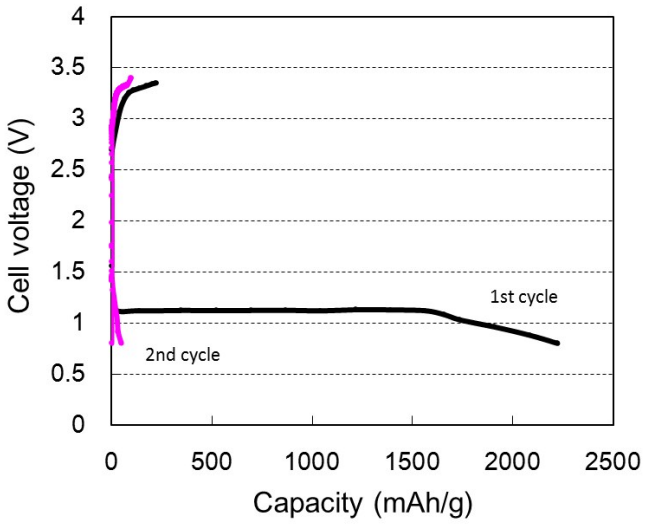

Figure S16. Discharge/charge cycles of Ca-O_2 battery using $Ca(ClO_4)_2$-DEMETFSA electrolyte. The concentration of $Ca(ClO_4)_2$ was 0.1 mol/L.